Volume 14, Issue 1, Page 13-20, 2025 https://doi.org/10.46810/tdfd.1531667 Research Article

BİNGÖL UNIVERSITY

Türk Doğa ve Fen Dergisi
Turkish Journal of Nature and Science
www.dergipark.gov.tr/tdfd

Impact of Different Cu Sources on the Structure, Surface Morphology, Optical and Photocatalytic Characteristics of Sol-Gel Derived CuO Thin Films

Sultan GÖKTAŞ[1*], Gülsen ŞAHİN[2]

[1] Harran University, Faculty of Arts and Science, Department of Chemistry, Şanlıurfa, Türkiye
[2] Adiyaman University, Faculty of Education, Department of Mathematics and Science Education, Adıyaman, Türkiye
Sultan GÖKTAŞ ORCID No: 0009-0000-7084-9710
Gülsen ŞAHİN ORCID No: 0000-0003-4891-041X

**Corresponding author: sultangoktas@harran.edu.tr*

(Received: 12.08.2024, Accepted: 01.12.2024, Online Publication: 26.03.2025)

Keywords
Thin film, Sol-gel, CuO, Cu-source, Band gap, Photocatalytic efficacy

Abstract: In this study, the impact of different Cu sources has been scrutinized on the structure, surface morphology, optical, and photocatalytic properties of CuO thin films, synthesized by sol-gel dip coating have been investigated. X-ray diffraction (XRD), scanning electron microscopy (SEM), energy dispersive spectroscopy (EDS) mapping, and UV–Vis spectroscopy were utilized to scrutinize them. The XRD patterns showed that the CuO films had a monoclinic CuO phase with a polycrystalline nature and their crystalline quality depended on the used Cu-source. Comparatively, the highest crystalline quality was observed for CuO film derived from the Cu-acetate source. The EDS and elemental mapping analysis exhibited the presence of Cu and O atoms within the film composition, randomly distributed on the film facets. As observed from the SEM analysis, the surface morphologies and grain sizes of CuO films were mainly changed by the Cu chemical source used. Variation in UV–Vis absorbance reflects different surface morphology and defect levels as the Cu-source was changed. The synthesized nanostructured CuO thin films showed highly varied photocatalytic activities and degradation rate of methylene blue dye solution under solar radiation. Among all synthesized CuO thin films, derived by using a Cu-chlorite source showed the highest photocatalytic efficacy within 150 min.

Farklı Cu kaynaklarının sol-jel ile türetilmiş CuO ince filmlerin yapısına, yüzey morfolojisine, optik ve fotokatalitik özelliklerine etkisi

Anahtar Kelimeler
İnce film, Sol-jel, CuO, Cu-kaynağı, Yasak band, Fotokatalitik verim

Öz: Bu çalışmada, sol-jel daldırarak kaplama yöntemi ile sentezlenen CuO ince filmlerin yapısı, yüzey morfolojisi, optik ve fotokatalitik özelliklerine farklı bakır kaynaklarının etkisi incelenmiştir. X-ışını kırınım difraksiyonu (XRD), taramalı elektron mikroskobu (SEM), enerji dağılımlı spektroskopi (EDS), haritalama ve UV-Vis spektroskopisi gibi çeşitli analiz yöntemleri onların özelliklerini incelemek için kullanılmıştır. XRD desenleri, CuO filmlerinin polikristal yapıya sahip monoklinik CuO fazına sahip olduğunu ve kristal kalitesinin büyük ölçüde kullanılan Cu kaynağına bağlı olduğunu gösterdi. Karşılaştırmalı olarak, en yüksek kristal kalitesi, Cu-asetat kaynağından türetilen CuO filmi için gözlemlendi. EDS ve element haritalama analizleri film bileşiğinde, film yüzeyine rastgele dağılan Cu ve O atomlarının varlığını gösterdi. CuO filmlerinin yüzey morfolojileri ve tane boyutları, SEM analizlerinden gözlemlendiği gibi, esas olarak kullanılan Cu kimyasal kaynağına göre değişti. UV-Vis soğrulma spektrumundaki değişiklik, Cu kaynağı değiştikçe farklı yüzey morfolojilerini ve kusur seviyelerini yansıtır. Sentezlenen nanoyapılı CuO ince filmleri, oldukça değişken fotokatalitik aktiviteler ve güneş ışınımı altında metilen mavisi çözeltisinin bozunumun oranları gösterdi. Sentezlenen tüm CuO ince filmleri arasında Cu-klorit kaynağı kullanılarak üretilen film, 150 dakikada en yüksek fotokatalitik verimi gösterdi.

1. INTRODUCTION

In the last decade, there has been a critical excursion to improve particularly well-organized, affordable, durable, safe photocatalysts and catalysts for large plate degradation of detrimental azo dyes and nitro aromatic compositions from wastewater [1-3]. It is reported that among all the metal oxide-based semiconductors ZnO and TiO_2 are the most explored photocatalysts to remove harmful organic pollutants within the water [4-5]. Reduced employment of sunlight arising from the wide optical band gaps of ZnO and TiO_2 restrict their efficacy as photocatalysts [6]. To overcome this limitation narrow optical band gap semiconductors viz. CuO and Cu_2O have acquired profound notice. Especially, the uniqueness of CuO nanoparticles is even though they are metallic in bulk they behave like semiconductors when they are in nanosize. In addition, the main reason for selecting CuO among other transition metals oxides is its semiconductivity, providing the usability in optoelectronic devices. Furthermore, Copper (Cu) is ample in nature in an immersion of approximately 60 g per ton and durable on the Earth's crust and the nanosized CuO, having relatively smaller size and larger surface area to volume ratio, showing better photocatalytic and antimicrobial activity compared to the other metal oxides.

CuO is a semiconductor known as p-type. This semiconductor can be found in three separate phases such as CuO, Cu_2O, and Cu_4O_3 [7-8]. Among these phases, CuO, which is the most likely to be found, crystallizes in a monoclinic structure. The lattice parameters vary as a=4.684 Å, b=3.425 Å, c=5.129 Å and β=99.28°. It has also been reported that the band gap of this phase is around 2.1 eV [9]. It has also been observed that the nanoscale forms of the structure have high absorption but low transmittance (20 %) in the visible region. In addition, the refractive index in the same region can vary between 2 and 2.5 [9]. Due to these superior properties, CuO is widely used in various applications such as solar cells, lithium-ion batteries, gas sensors, and glucose sensors [10]. Moreover, the physicochemical characteristic of their nanostructures makes them promising materials for possible optoelectronic and photocatalytic applications [11-12]. CuO nanocrystalline thin films can be used for the large-scale diminishing of pollutants from wastewater and several types of solar cells.

CuO thin films are frequently preferred in several applications due to their properties such as Cu components being abundant in nature, being environmentally friendly, and non-toxic. Various thin film production methods have been used to synthesize CuO thin films. These methods can be listed as follows; chemical vapor deposition, electrodeposition, thermal oxidation, reactive magnetron sputtering, molecular beam epitaxy, ultrasonic spray pyrolysis, and also sol-gel. Among these methods, the sol-gel technique is potentially more preferred due to its useful, simple, uncomplicated, non-complicated, and economical method for obtaining CuO thin films Additionally, the dip coating process represents an effective method for coating large surfaces [13-17].

The photocatalytic performance of semiconductor thin film photocatalysts is highly upon on agents viz. facet morphology, crystallite/grain size, degree of crystallinity, active surface area, etc. [18–20]. For example, the photocatalytic behavior of CuO nano-whiskers thin film was reported by Mukherjee et al. [21]. In the reported study, the CuO nano-whiskers thin film showed a photocatalytic efficiency of 84 % for degradation of Rhodamine B (RhB) within 260 min under visible light. Similarly, CuO thin films having star like morphology showed 95 % photocatalytic efficiency in 210 min towards the photodegradation of methylene blue (MB) [22]. On the other hand, in nanowire-shaped CuO thin films, the MB removal efficacy reached 95.6 % in 210 min as reported by Wang et al [23]. It was reported that CuO nanostructures with flower-like shapes exhibited a high MB degradation efficiency of 98 % in 90 min [24]. Recently, the effect of annealing temperature on the photodegradation ability of CuO has been examined. The CuO degradation efficiency towards malachite green and MB was improved with increased annealing temperature due to the enhanced surface area of the CuO thin films [25]. More recently, Komaraiah et al. [26] have prepared CuO thin films having different film thicknesses, derived by spin coater technique, for degradation of the MB and Methyl orange under visible light. The maximum photocatalytic efficiency of 89.91 % was reported.

Herein, CuO thin films with different surface morphology were produced by sol-gel dip coating process using different Cu sources. The influences of the Cu-sources on the morphological, structural, optical, and photocatalytic behavior for the degradation of MB dye in water have been examined. According to our best knowledge, the influence of the different Cu sources on the above-mentioned properties has not been scrutinized yet. Therefore, investigating the influences of different Cu-sources on the morphological, structural, optical, and photocatalytic properties is highly attractive to get highly efficient, economical, stable, and reusable photocatalytic thin films for large-scale remove of organic pollutants and hazardous chemicals from wastewater.

2. MATERIAL AND METHOD

2.1. Synthesis Method of CuO Thin films

CuO thin films were grown by sol-gel dip coating method using 2-methoxyethanol ($C_3H_8O_3$), ethanolamine (C_2H_7NO), and different zinc sources such as copper (II) acetate monohydrate ($(CH_3COO)_2Cu.H_2O$), nitrate trihydrate ($Cu(NO_2).3H_2O$), and chlorite dihydrate ($CuCl_2 .2H_2O$). All used chemicals were analytically graded and not subjected to further purification, were used to grow the main solution of the thin films. To prepare different film solutions, 0.05 M of each of these zinc sources were separately dissolved in $C_3H_8O_3$ using a magnetic stirrer with a hot plate at room temperature for 30 min. Then a certain amount of the $C_3H_8O_3$ was added to each solution as a stabilizer. The final solutions were aged for 24 h overnight with continuous stirring on the hot plate at room temperature using magnetic rotators. The obtained last mixtures are completely homogeneous and transparent

(no suspended or insoluble particles were observed in them) and also have various coloring (blue, green, and pink) due to using different Cu-salt sources. Afterward, the mixture solutions were poured into 50 ml wells for coating on the glass substrates that were previously cleaned by washing them in an ultrasonic acetone and methanol bath. Finally, the clean glass substrates were deposited by a dip coating method using the final mixture solutions at 400 ºC. The deposited film samples were sintered in the air atmosphere at 500 ºC for 1 h. From now the deposited film samples will be called Cu-acetate, Cu-nitrate, and Cu-chlorite in this text according to used copper (II) acetate monohydrate ($(CH_3COO)_2Cu.H_2O$), nitrate trihydrate ($Cu(NO_2).3H_2O$), and chlorite dihydrate ($CuCl_2 .2H_2O$) chemical sources.

2.2. Characterization Techniques of CuO Thin Films

X-ray diffraction, XRD (Rigaku Ultima III (40 kV, 40 mA, and 1.54 A°)) diffractometer was used to check crystal phases and impurities in CuO thin films obtained by sol-gel dipping technique. Scanning electron microscopy, SEM (Zeiss Evo 50, 200 kV) was used for surface analysis and determination of the film thickness (from a cross-section of the film samples) of CuO thin samples. EDX (energy dispersion X-ray spectrophotometry) and elemental mapping methods were used to perform elemental analysis in the films. On the other hand, a UV-Vis spectrophotometer was used to determine the optical properties of the films (300-1100 nm wave) and to take absorption measurements of methylene blue (MB) dye after the photocatalytic process.

2.3. Photocatalytic Measurements of CuO Thin Films

To prepare the MB solution, 1.25 mg/L MB was dissolved in 100 ml of pure water using a magnetic stirrer at room temperature. It was then stirred until properly dissolved. The pH of the mixture (using a Hanna pH meter (HI2211 pH/ORP meter)) was regulated by the desired NaOH content. According to studies in the literature, MB undergoes best photodegradation at pH = 11 [27, 28].

The photocatalytic degradation behavior of MB was assessed in water under 200 W visible light using CuO thin films as a photocatalyst. For this study, 1.25 mg/L of MB solution in 100 mL of deionized water was made ready in a flask made up of glass and synthesized CuO thin films were submerged in this solution. This vial was left in a dark condition for 30 min to get an equilibrium of adsorption–desorption. Then it was exposed to sunlight for 30 min intervals. The absorption of MB solutions before and after various 30-min irradiation times was guided and examined using a UV–Vis spectroscopy (PerkinElmer Lambda 25) coupled to the distinctive absorption of the MB top at 664 nm. The efficacy of the CuO nanocrystalline photocatalysts was computed using the formula of $\eta = [(1-(C/C_0))]x100$.

Here, C_0 and C are the main absorption peaks of MB and represent the intensity of MB before and after photocatalysis, respectively.

3. RESULTS

3.1. Structural and Morphological Studies

The XRD patterns of CuO thin films obtained using different chemical sources are given in Figure 1. The XRD patterns showed that CuO thin films crystallize in the monoclinic CuO phase and crystallization (crystallite size) varies depending on the Cu chemical source used. Polycrystalline and nanostructured CuO thin films with (110), (002), (111), ($\bar{2}02$), (021), ($\bar{1}13$), and (220) miller indices (matched well with JCPDF card #89-5899, and ICSD card #087126) and preferred to crystallize at a higher rate along the plane side of (002) [2].

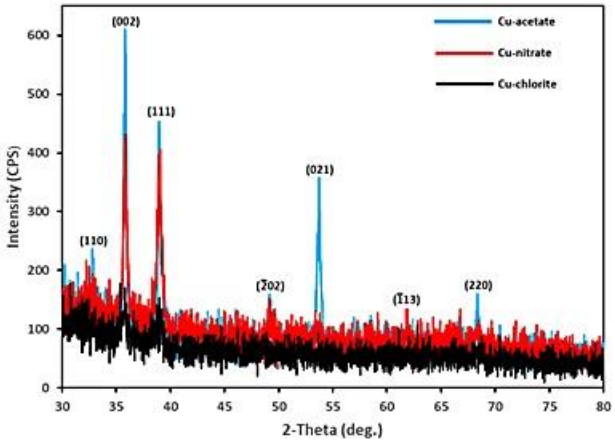

Figure 1. XRD patterns of CuO thin film samples Cu-acetate, Cu-nitrate, and Cu-chlorite

The crystallite size was calculated from the chief x-ray diffraction peak, having high peak intensity, at 2θ = 35.70°- 35.70° using Scherrer's formula [13].

$$D = 0.9\lambda/\beta\cos(\theta) \quad (1)$$

where β is FWHM, λ is the wavelength of the incident X-ray, and θ is the diffraction angle. The micro-strain ($\varepsilon = \beta\cos(\theta)$), and dislocation density ($\delta=1/D^2$) of the CuO films were evaluated [5] and given in Table 1.

Table 1. The full-width half-maximum, diffraction angle, crystallite size, dislocation density, micro-strain, and lattice parameter of the prepared CuO nanocrystalline thin film samples Cu-acetate, Cu-nitrate, and Cu-chlorite.

Cu-source	FWHM (β°)	2θ(deg.)	D_{hkl}(nm)	$\delta x10^{-3}$	ε x 10^{-3}	a (Å)
Acetate	0.28	35.70	30.00	11.11	2.640	4.779
Nitrate	0.43	35.76	19.53	26.21	4.243	4.729
Chlorite	0.78	35.80	10.76	86.37	7.919	4.717

It was observed that the examined SEM surface morphologies of nano-structured CuO thin films varied depending on the type of Cu chemical source used (Fig. 2a-c). Although the surfaces of these films are dense and homogeneous with some cracks and surface roughness have been observed. It can be seen from Fig.2a that the nanostructured CuO thin film prepared with copper acetate has denser and larger grains than those prepared with other Cu-source chemicals (Cu-nitrate and Cu-chlorite).

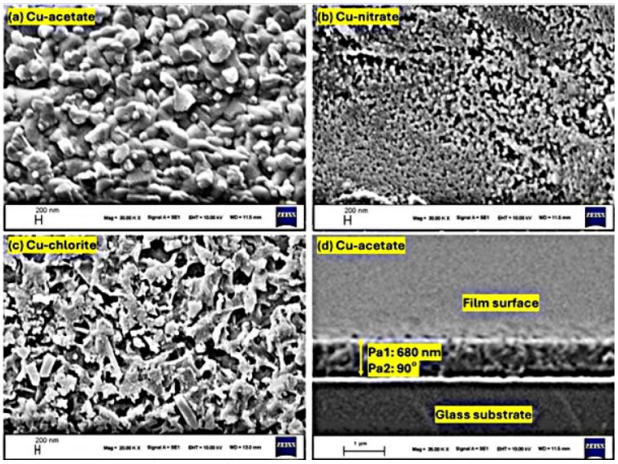

Figure 2. SEM images of the synthesized CuO thin film samples Cu-acetate (a), Cu-nitrate (b), Cu-chlorite (c), and the film thickness of Cu-chlorite film sample.

EDX and mapping technique results are presented in Fig. 3a-d. EDX spectra of the Cu-acetate film sample was given in Fig. 3a and confirmed the presence of Cu (51.40 at. %) and O (48.60 at. %) atoms in the film samples (Fig. 3a). The presence of the Au atom is due to the conductive contact used. In addition, it is understood from the mapping results that Cu (red) and O (green) atoms are distributed homogeneously on the film facet (Fig. 3b). The distribution of the Cu and O atoms was also given in different images as seen in Fig. 3c and 3d, respectively. Furthermore, the black spots or other colors show that the elements do not organize or flow in only mark contentment.

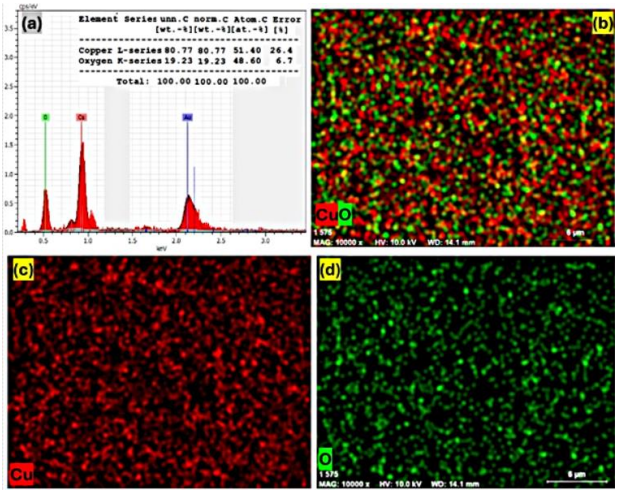

Figure 3. EDX spectra of the synthesized Cu-chlorite film sample (a), total color mapping (b), and color mapping of Cu (c) and O (d).

3.2. UV-Vis Measurements

UV–Vis absorption spectroscopy was carried out to monitor the optical response of the deposited CuO nanostructured thin film. The absorbance spectra of the prepared with acetate, nitrate, and chloride starting chemical sources, depending on wavelength and starting chemical type, are given in Fig. 4a. Tauc plots were utilized for the resolving of band gap values of CuO nanocrystalline films [32, 33]. The estimated bandgap values calculated as 1.51, 1.72 eV, and 1.66 eV for the Cu-acetate, Cu-nitrate, and Cu-chlorite thin films, respectively (see Fig. 4b).

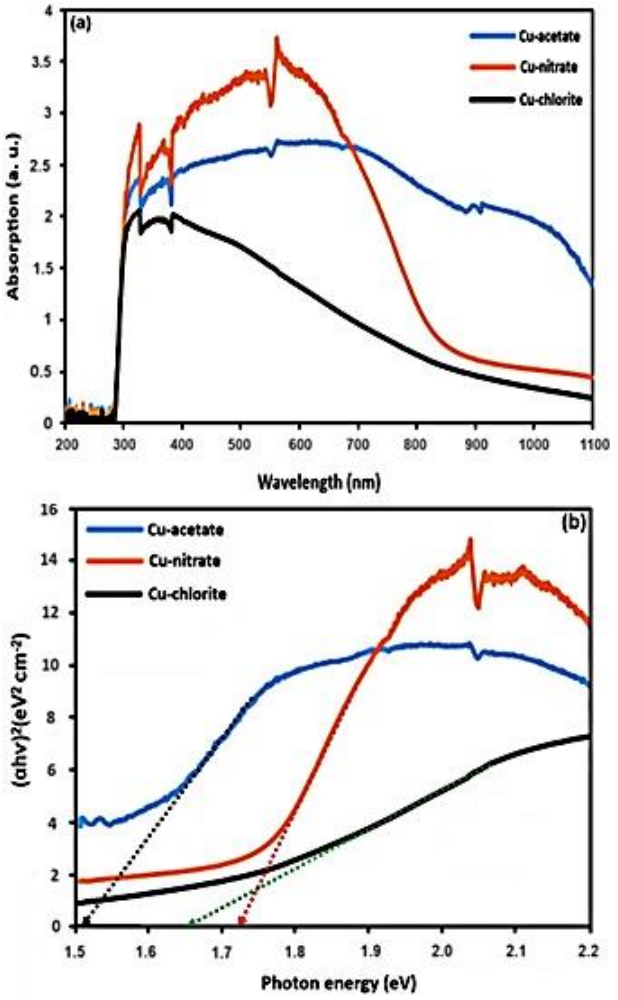

Figure 4. (a) UV–Visible absorption spectra of the synthesized CuO thin film samples Cu-acetate, Cu-nitrate, and Cu-chlorite, (b) Tauc curves of the synthesized samples.

3.3. Evaluation of Photocatalytic Studies

Photocatalytic actions of CuO thin films were scrutinized by degradation of MB dye under visible light radiation. Visible light radiation-induced swaps in the absorption spectrum of MB solution both for CuO thin film samples Cu-acetate, Cu-nitrate, and Cu-chlorite are given in Fig. 5 (a–c). The absorption at 664 nm is moderately impaired with increasing exposure time. The synthesized sample Cu-chlorite was observed to be the best photocatalyst and partially degraded MB in 150 min.

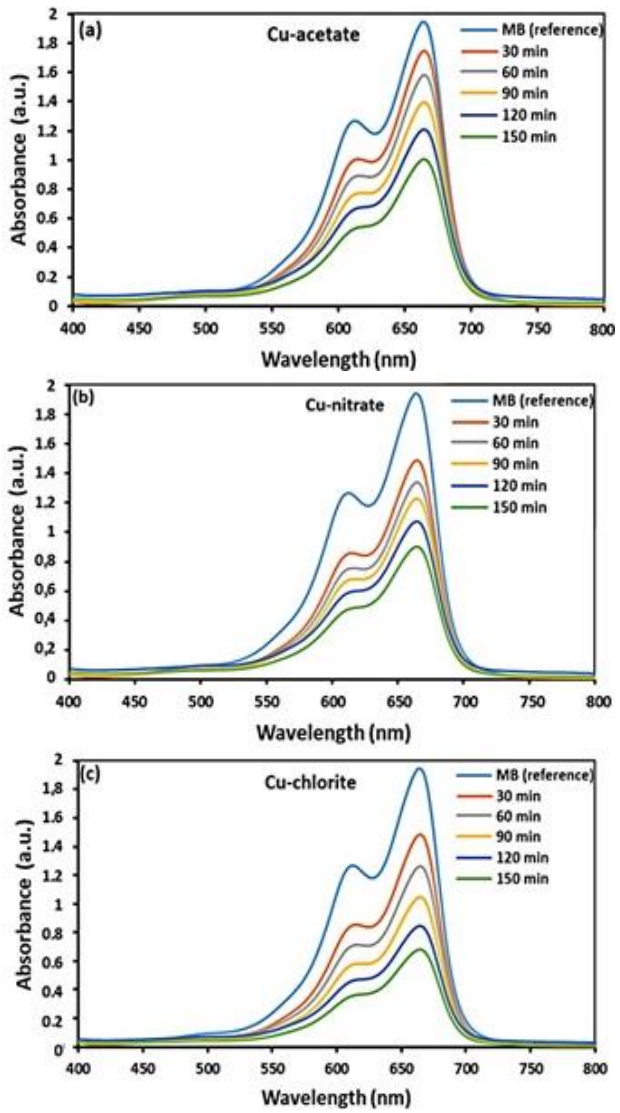

Figure 5. Absorption spectra of MB in the existence of CuO thin film samples Cu-acetate (a), Cu-nitrate (b), and Cu-chlorite (c).

Accordingly, the highest degradation ratio was observed in Fig. 5c. So, the highest MB degrade ratio was observed for the Cu-chlorite photocatalyst as its highest active surface area due to having nanorods-like shaped facet morphology and having relatively lower crystallite size. Therefore, the changes may be nearly same but the intensity variation is different by time for the used 3 samples.

The kinetics (C/Co versus time) of the photocatalytic degradation of MB by the synthesized CuO samples are exhibited in Fig. 6 (a). As can be seen from it, the C/Co ratio reduces according to the Cu-acetate, Cu-nitrate, and Cu-chlorite samples. A relatively fast reduction has been observed for the Cu-chlorite sample.

The first order rate constant for the degradation of MB was estimated by utilizing the formula [34]:

$$C/C_0 = \exp(-kt) \qquad (2)$$

where k reflects the rate constant, C and C_0 represent the first and final concentration of dye, respectively.

The rate constants for the degradation of MB by the CuO thin film photocatalysts such as Cu-acetate, Cu-nitrate, and Cu-chlorite are computed as 0.0078, 0.009 and 0.0114 min^{-1}, respectively (Fig. 6(b)). The variation in the efficacy of CuO thin films for MB degradation with the radiation time is exhibited in Fig. 6(c). The computed values according to the efficacy formula, described in our previous ref [34] are 52.50, 57.00, and 68.50 % for the Cu-acetate, Cu-nitrate, and Cu-chlorite film samples, respectively. These results show that CuO nanostructured thin film prepared by Cu-chlorite precursor is the most efficient photocatalyst for the solar-driven degradation of MB dye in water.

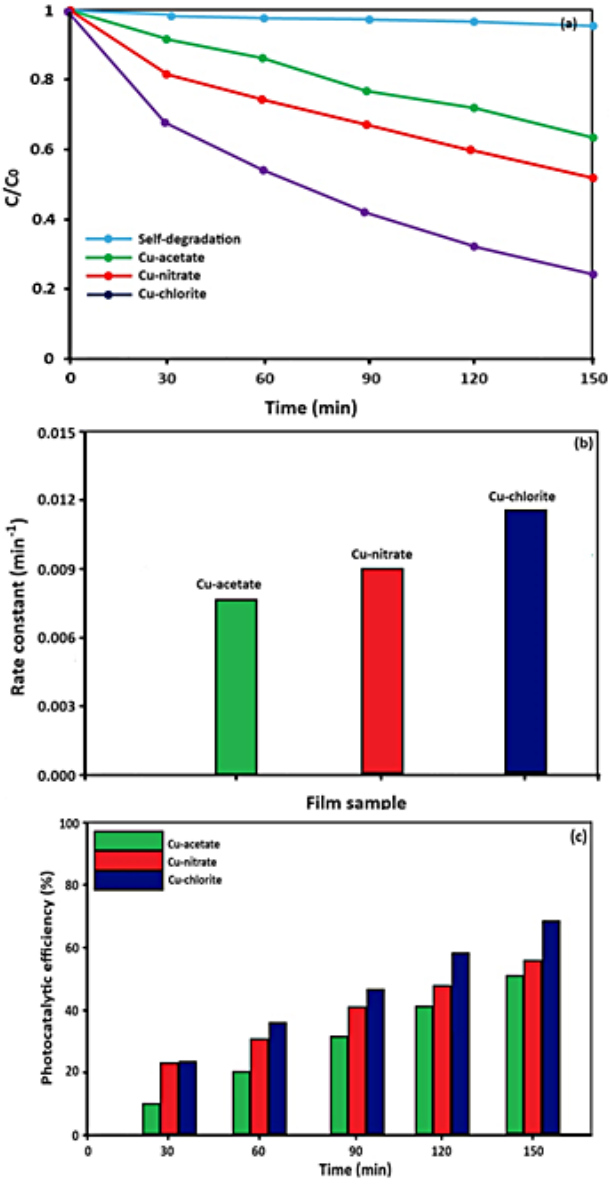

Figure 6. Variation in C/C_0 of MB with time for different photocatalysts under sunlight illumination (a), rate constant (b), and efficiency (c) of the prepared photocatalysts for the degradation of MB.

The rate constants for the degradation of MB by the CuO thin film photocatalysts such as Cu-acetate, Cu-nitrate, and Cu-chlorite are computed as 0.0078, 0.009 and 0.0114 min^{-1}, respectively (Fig. 6(b)). The variation in the efficacy of CuO thin films for MB degradation with the radiation time is exhibited in Fig. 6(c). The computed values according to the efficacy formula, described in our

previous ref [34] are 52.50, 57.00, and 68.50 % for the Cu-acetate, Cu-nitrate, and Cu-chlorite film samples, respectively. These results show that CuO nanostructured thin film prepared by Cu-chlorite precursor is the most efficient photocatalyst for the solar-driven degradation of MB dye in water.

4. DISCUSSION AND CONCLUSION

The D reduces by changing the Cu-source type and the D of the Cu-acetate sample has the highest value among all the prepared film samples. The ε and δ values of the film samples decrease by enhancement of the D values reflecting deterioration of the crystalline quality of the film samples with varying Cu-source type. A slight decrement in a lattice constant is observed due to the reduction of the D.

It is seen in the SEM measurement results that the grain sizes vary between approximately 100-400 nm. The observed different grain shapes were mainly attributed to the used Cu-source. The trend in grain size variation is nearly the same with the analysis of XRD showing a good agreement between the SEM and XRD results. However, it was determined that the grain sizes observed by SEM were larger than the crystal size calculated based on XRD data. This is due to grain sizes containing more than one crystallite [29]. Moreover, the thickness of the produced films is about 680 nm as seen in Fig. 2d, which corresponds to the Cu-acetate film sample.

According to the optical absorption of the films varies depending on the type of starting chemical exhibiting the starting chemical sources influence the light-capacity of the produced CuO thin film samples. The highest absorption in the visible region was observed for the film sample prepared with Cu-nitrate chemical compared to the other film samples. On the other hand, among all the film samples the highest absorption at wavelengths higher than the visible region was observed in the film prepared with Cu-acetate precursor chemical. While the increase in optical absorption is directly related to the structure of the material, it is also closely related to the increase in crystal defects and the rate of crystallization [8, 30, 31]. It is understood from the absorption spectra that the absorption edge of the films varies depending on the type of starting chemical used.

The film samples show a narrow bandgap and permit good solar spectral absorption, leading to an increment of solar energy driven photocatalytic efficiency. The E_g values are in good agreement with previous reports on the CuO thin films [34].

The variations in the Figure 5 are depended on several factors and the decreasing in their intensity reflects the degradation of the MB within the MB dye solution. These factors are highly depending on the surface morphology and the crystallite size of the photocatalyst as well as the defect concentrations. It is expected the variations need to be same but the intensity of them should be decreased by time, reflecting degraded MB contents monotonically.

The possible procedure of dye degradation by CuO nanocrystalline thin film photocatalyst is diagrammatically exhibited in Fig. 7. In this mechanism, electrons are excited to the conduction band depending on the radiation of sunlight. The photo-induced electrons react with the O_2 absorbed creating superoxide radicals ($*O^{-2}$), whereas the holes interact with H_2O molecules and facet hydroxyl groups generating hydroxyl radicals ($*OH$). The ($*O^{-2}$) and $*OH$ radicals are accountable for the noticed dye degradation [35, 36].

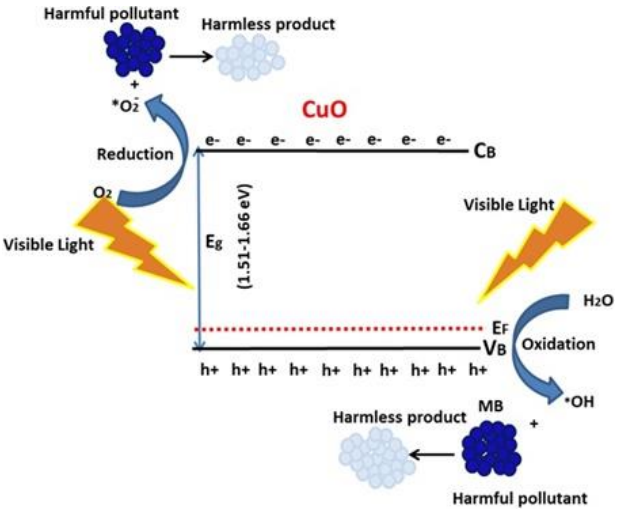

Figure 7. Proposed process of photocatalytic degradation of organic MB dye by CuO thin film.

The investigated characteristics such as optical, structural, and morphological have major influences on the photocatalytic activity of CuO nanostructures. The mean grain/crystallite size of CuO nanostructured thin film upon the sintering temperature and time [37–39]. The E_g, light absorption capability, crystallization and the facet area of CuO nanocrystalline thin films modify their photocatalytic activity.

Reduction in the E_g results in the uncomplicated movement of electrons in the CuO nanocrystalline, leading to an upgrade in the photocatalytic activity. Sahu et al. [25] reported that the CuO nanostructured thin film sintered at 400 °C exhibited better photocatalytic behavior as compared to other samples because of its smaller band gap and higher light absorption ability. In the present study, different surface areas due to different crystallite/grain sizes, narrow band gap, and increased use of light assisting better adsorption of MB dye molecule in the CuO nanocrystalline film synthesized by Cu-chlorite source are chiefly accountable for its relatively enhanced photocatalytic efficacy toward the degradation of MB dye in water.

In conclusion, the nanocrystalline CuO thin films were prepared using sol-gel dip coating technique and different Cu-chemical sources under air ambient. Depending on the used Cu-chemical sources, notable moderations in the surface morphology, optical, structural, and photocatalytic activity of CuO nanocrystalline thin film were found. CuO nanocrystalline thin film synthesized by Cu-chlorite source showed superb behavior for the photocatalytic debasement of MB dye in water. The

degradation of MB in the existence of Cu-chlorite nanocrystalline thin film sintered at 500 °C occurs in 150 min beneath sunlight radiation. The enhanced photocatalytic activity of the Cu-chlorite nanocrystalline thin film is ascribed to its relatively high surface area/low crystallite size, narrow E_g (1.66eV), refined usage of sunlight, and increased adsorption of MB dye owing to the increased formation of relatively higher active surface area of Cu-chlorite nanocrystalline at the film facet. The synthesized CuO nanocrystalline thin films can be used in photocatalytic degradation of harmful organic contaminants from wastewater because of their handle, economic, environmentally friendly, and stability.

Acknowledgement

The authors are grateful to the Laboratory team of Department of Physics, Faculty of Arts and Science for guiding the author during this scientific research at Harran University.

REFERENCES

[1] Kwan I, Mapstone J. Visibility aids for pedestrians and cyclists: a systematic review of randomised controlled trials. Accid Anal Prev. 2004;36(3):305-12.

[2] Lachheb H, Puzenat E, Houas A, Ksibi E, Elaloui E, Guillard C, et al. Photocatalytic degradation of various types of dyes (alizarin S, crocein orange G, methyl red, congo red, methylene blue) in water by UV-irradiated titania. Appl. Catal B: Environ. 2002; 39:75-90.

[3] Goktas S, Goktas A. A comparative study on recent progress in efficient ZnO based nanocomposite and heterojunction photocatalysts: A review. J Alloy Compd. 2021; 863: 158734.

[4] Banazadeh A, Salimi H, Khaleghi M, Haghighi SS. Highly efficient degradation of hazardous dyes in aqueous phase by supported palladium nano catalyst-a green approach. J Environ Chem Eng. 2016; 4:2178-2186.

[5] Göktaş S, Aslan F. Kimyasal çöktürme yöntemiyle belirli karboksilik asitlerden organosiklotrifosfazen üretimi ve kimyasal özellikleri. Harran üniversitesi mühendislik dergisi, 2019; 4(3):19-28.

[6] Goktas A, Modanlı S, Tumbul A, Kilic A. Facile synthesis and characterization of ZnO, ZnO: Co, and ZnO/ZnO: Co nano rod-like homojunction thin films: Role of crystallite/grain size and microstrain in photocatalytic performance. J Alloy and Compd. 2022; 893:162334.

[7] Faisal M, Khan SB, Rahman MM, Jamal A, Asiri AM, Abdullah MM. Smart chemical sensor and active photo-catalyst for environmental pollutants. Chem Eng J. 2011; 173:178-184.

[8] Shariffudin SS, Khalid SS, Sahat NM, Sarah MSP, Hashim H. Preparation and characterization of nanostructured CuO thin films using sol-gel dip coating, IOP Conf Series: Mater. Sci. Eng. 2015:99;012007.

[9] Vikas P, Datta J, Shailesh P, Manik C, Prsad G, Sanjay P. Nanocrystalline CuO thin films for H2S monitoring: microstructural and optoelectronic characterization, J. Sens. Tech. 2011;1(2):36.

[10] Lidia A, Davide B, Manuel B, Gregorio B, Cinzia S, Eugenio T. A sol–gel approach to nanophasic copper oxide thin films, Thin Solid Films. 2003; 442:48–52.

[11] Jessica LR, Jorge M, Guerrero-V, María de LMG, Francisco S, Aguirre-Tostado et al. G, Gutiérrez H., Israel M-S., Amanda, CC. Optical and microstructural characteristics of CuO thin films by sol gel process and introducing in non-enzymatic glucose biosensor applications. Optik. 2021; 229:166238.

[12] Zaman S, Zainelabdin A, Amin G, Nur O, Willander M. Efficient catalytic effect of CuO nanostructures on the degradation of organic dyes. J Phys Chem Solids 2012; 73:1320-1325.

[13] Xu C, Sun J, Gao L, J Power Sources 2011;196:5138.

[14] Goktas S, Tumbul A, Goktas A. Growth technique–induced highly c-axis-oriented ZnO: Mn, ZnO:Fe and ZnO:Co thin films: a comparison of nanostructure, surface morphology, optical band gap, and room temperature ferromagnetism. J Supercond Nov Magn 2023;36: 1875.

[15] Bayansal F, Taşköprü, T Şahin B, Çetinkara HA. Effect of cobalt doping on nanostructured CuO thin films. Metall Mater Trans A. 2014; 45:3670.

[16] Şahin G, Göktaş S, Calculation of structural parameters and optical constants of size dependent ZrO2 nanostructures. GJES. 2024; 10(1)114–124.

[17] Goktas A, Role of simultaneous substitution of Cu2+ and Mn^{2+} in ZnS thin films: defects-induced enhanced room temperature ferromagnetism and photoluminescence. Phys. E: Low-Dimens. Syst. Nanostructures. 2020; 117:113828.

[18] Goktas A, High-quality solution-based Co and Cu co-doped ZnO nanocrystalline thin films: Comparison of the effects of air and argon annealing environments. J Alloy Compd. 2018;735: 2038-2045.

[19] Bensouici F, Bououdina M, Dakhel AA, Tala-Ighil R, Tounane M, Iratni A, et al. Optical, structural and photocatalysis properties of Cu-doped TiO2 thin films. Appl. Surf. Sci. 2017; 395:110–116.

[20] Goktas A, Modanlı S, Tumbul A, Kilic A. Facile synthesis and characterization of ZnO, ZnO: Co, and ZnO/ZnO: Co nano rod-like homojunction thin films: Role of crystallite/grain size and microstrain in photocatalytic performance. J. Alloy Compd. 2022; 893:162334.

[21] Mikailzade F, Önal F, Maksutoglu M, Zarbali M, Göktaş A. Structure and magnetization of polycrystalline La0.66Ca0.33MnO3 and La0.66Ba0.33MnO3 films prepared using sol-gel technique. J Supercond Nov Magn. 2018; 31:4141–4145.

[22] Mukherjee N, Show B, Maji SK, Madhu U, Bhar SK, Mitra BC, et al. CuO nano-whiskers: electrodeposition, Raman analysis, photoluminescence study and photocatalytic activity, Mater Lett. 2011; 65:3248–3250.

[23] Wang Y, Jiang T, Meng D, Yang J, Li Y, Ma Q, et al. Fabrication of nanostructured CuO films by

electrodeposition and their photocatalytic properties, Appl Surf Sci. 2014;317:414–421.
[24] Wang Y, Jiang T, Meng D, Jin H, Yu D. Controllable fabrication of nanowirelike CuO film by anodization and its properties. Appl Surf Sci. 2015; 349:636–643.
[25] Gao F, Zhu L, Li H, Xie H. Hierarchical flower-like CuO film: one-step room temperature synthesis, formation mechanism and excellent optoelectronic properties. Mater Res Bull. 2017; 93:342–351.
[26] Kavita S, Shipra Choudhar S, Khan A, Akhilesh P, Satyabrata M. Thermal evolution of morphological, structural, optical and photocatalytic properties of CuO thin films. Nano-Struct. Nano-Obj. 2019; 17:92–102.
[27] Komaraiah D, Sayanna R. Structural, optical properties and photocatalytic activity of spin-coated CuO thin films. Adv Nat Sci: Nanosci. Nanotechnol. 2023; 14:015006.
[28] Göktaş S, Sahin G. Methylene blue concentration and pH-induced photocatalytic degradation of methylene blue without photocatalyst under visible light. Inter. J Adv Nat. Sci. Eng. Res. 2023;7(6):176-181.
[29] Tumbul A, Aslan E, Göktaş A, Mutlu IH, Arslan F, Aslan F. Chemically derived quinary Cu2Co1–xNaxSnS4 photon absorber material and its photocatalytic application. Appl Phys A. 2024;130:225.
[30] Goktas A, Aslan F, Mutlu IH. Annealing effect on the characteristics of $La_{0.67}Sr_{0.33}MnO_3$ polycrystalline thin films produced by the sol–gel dip-coating process. J Mater Sci: Mater Electron. 2012; 23:605–611.
[31] Sekhar CR, Preparation of copper oxide thin film by the sol–gel-like dip technique and study of their structural and optical properties. Sol. Energy Mater. Sol. Cells. 2001; 68(3–4): 307.
[32] Goktas A, Aslan F, Tumbul A. Nanostructured Cu-doped ZnS polycrystalline thin films produced by a wet chemical route: the influences of Cu doping and film thickness on the structural, optical and electrical properties. J Sol-Gel Sci Technol. 2015; 75:45.
[33] Wang Z, Pischedda V, Saxena SK, Lazor P. X-ray diffraction and Raman spectroscopic study of nanocrystalline CuO under pressures, Solid State Commun. 2002; 121:275–279.
[34] Goktas A, Sol–gel derived Zn1−xFexS. Diluted magnetic semiconductor thin films: compositional dependent room or above room temperature ferromagnetism, Appl. Surf. Sci. 2015; 340:151-159.
[35] Göktaş S, Synergic effects of pH, reaction temperature, and various light sources on the photodegradation of methylene blue without photocatalyst: a relatively high degradation efficiency. Chem Africa. 2024; 1-13.
[36] Maryam K-S, Alireza N-E. Comparative study on the increased photoactivity of coupled and supported manganese-silver oxides onto a natural zeolite nanoparticle. J Mol Catal. A: Chem. 2016;(418–419):103-114.
[37] Goktas S, Metilen mavisi organik boyasinin güneş ışığında katalizörsüz yıkımı. Inter. Conf. Eng. Nat. Soc. Sci. 2023; 1, 364-367.
[38] Huang H, Tu S, Zeng C, Zhang T, Reshak HA, Zhang Y, Macroscopic polarization enhancement promoting photo-and piezoelectric-induced charge separation and molecular oxygen activation, Angew Chem Inter Ed. 2017;56:11860–11864.
[39] Goktas A, Aslan F, Mutlu IH. Effect of preparation technique on the selected characteristics of Zn1−xCoxO nanocrystalline thin films deposited by sol–gel and magnetron sputtering. J. alloy compd. 2014; 615:765-778.
[40] Aslanoglu M, Goktas S, Karabulut S, Kutluay A. Cyclic voltammetric determination of noradrenaline in pharmaceuticals using poly (3-acetylthiophene)-modified glassy carbon electrode. Chem. Analityczna, 54(4), 643-653.